DdcA antagonizes a bacterial DNA damage checkpoint

**Peter E. Burby, Zackary W. Simmons and
Lyle A. Simmons** iD
*Department of Molecular, Cellular, and Developmental
Biology, University of Michigan, Ann Arbor, MI 48109,
USA.*

Summary

Bacteria coordinate DNA replication and cell division, ensuring a complete set of genetic material is passed onto the next generation. When bacteria encounter DNA damage, a cell cycle checkpoint is activated by expressing a cell division inhibitor. The prevailing model is that activation of the DNA damage response and protease-mediated degradation of the inhibitor is sufficient to regulate the checkpoint process. Our recent genome-wide screens identified the gene *ddcA* as critical for surviving exposure to DNA damage. Similar to the checkpoint recovery proteases, the DNA damage sensitivity resulting from *ddcA* deletion depends on the checkpoint enforcement protein YneA. Using several genetic approaches, we show that DdcA function is distinct from the checkpoint recovery process. Deletion of *ddcA* resulted in sensitivity to *yneA* overexpression independent of YneA protein levels and stability, further supporting the conclusion that DdcA regulates YneA independent of proteolysis. Using a functional GFP-YneA fusion we found that DdcA prevents YneA-dependent cell elongation independent of YneA localization. Together, our results suggest that DdcA acts by helping to set a threshold of YneA required to establish the cell cycle checkpoint, uncovering a new regulatory step controlling activation of the DNA damage checkpoint in *Bacillus subtilis*.

Introduction

The logistics of the cell cycle are of fundamental importance in biology. All organisms need to control cell growth, DNA replication, and the process of cell division. In bacteria the initiation of DNA replication is coupled to growth

rate and the cell cycle (Donachie and Blakely, 2003; Wang and Levin, 2009; Hill *et al.*, 2012; Westfall and Levin, 2017). Bacteria also regulate cell division in response to DNA replication status through the use of DNA damage checkpoints (Lenhart *et al.*, 2012; Kreuzer, 2013). The models for the DNA damage response (SOS) were developed based on studies of *Escherichia coli* and subsequently extended to other bacteria. In these models, DNA damage results in perturbations to DNA replication and the accumulation of ssDNA (Friedberg *et al.*, 2006). RecA is loaded onto ssDNA (Anderson and Kowalczykowski, 1997; Churchill *et al.*, 1999; Ivancic-Bace *et al.*, 2003; Morimatsu and Kowalczykowski, 2003; Ivancic-Bace *et al.*, 2006), and the resulting RecA/ssDNA nucleoprotein filament induces the SOS response by activating auto-cleavage of the transcriptional repressor LexA (Slilaty and Little, 1987). LexA inactivation results in increased transcription of genes involved in DNA repair and the DNA damage checkpoint (Little *et al.*, 1981; Little and Mount, 1982; Lewis *et al.*, 1994; Au *et al.*, 2005; Goranov *et al.*, 2006). The DNA damage checkpoint is established by relieving the LexA-dependent repression of a cell division inhibitor that enforces the checkpoint by blocking cell division (Huisman and D'Ari, 1981; Huisman *et al.*, 1984; Kawai *et al.*, 2003; Mo and Burkholder, 2010). Once the checkpoint is established, the delay in cytokinesis provides the cell with enough time to repair and complete DNA replication, thereby ensuring a complete and accurate copy of the chromosome is segregated to both daughter cells. Over several decades of study, this overarching model has been consistently demonstrated among bacteria that contain a RecA and LexA-dependent DNA damage checkpoint mechanism (Erill *et al.*, 2007; Kreuzer, 2013).

Where the DNA damage response varies between bacteria is in the process that enforces and alleviates the checkpoint. In *E. coli* and closely related Gram-negative bacteria, the checkpoint is enforced by SulA, which is a cytoplasmic protein that acts by directly inhibiting formation of the FtsZ proto-filament blocking cell division (Huisman *et al.*, 1984; Bi and Lutkenhaus, 1993; Huang *et al.*, 1996; Mukherjee *et al.*, 1998; Trusca *et al.*, 1998). In many other bacteria the checkpoint is enforced by a small membrane-binding protein (Kawai *et al.*, 2003; Chauhan *et al.*, 2006; Ogino *et al.*, 2008; Modell *et al.*, 2011; 2014). In *Caulobacter crescentus*, the small membrane proteins
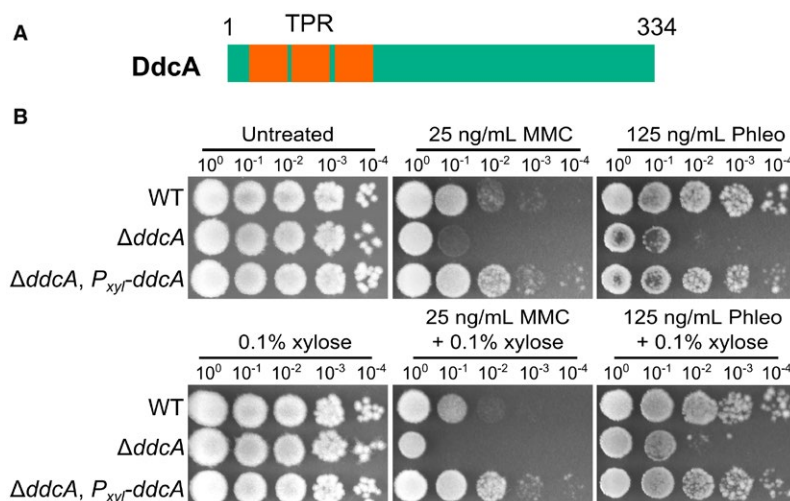
Fig. 1. Deletion of *ddcA* (*ysoA*) results in sensitivity to DNA damage.
A. A schematic of the DdcA protein. DdcA is predicted to have 334 amino acids and three tetratrichopeptide repeats at its N-terminus.
B. A spot titer assay in which exponentially growing cultures of *B. subtilis* strains WT (PY79), Δ*ddcA* (PEB357) and Δ*ddcA*, *amyE*::P$_{xyl}$-*ddcA* (PEB503) were spotted on the indicated media and incubated at 30°C overnight. [Colour figure can be viewed at wileyonlinelibrary.com]

SidA and DidA inhibit cell division through direct interactions with components of the essential cell division complex known as the divisome (Modell *et al.*, 2011; 2014). In other bacteria, the exact mechanism of checkpoint enforcement remains unclear. In the Gram-positive bacterium *Bacillus subtilis*, the checkpoint enforcement protein YneA inhibits cell division in response to DNA damage (Kawai *et al.*, 2003). YneA is a small protein containing a transmembrane domain as well as a LysM domain (Mo and Burkholder, 2010). A previous study found that several amino acids on one side of the transmembrane alpha helix are important for function, which led the authors to speculate that YneA may also interact with a component of the divisome (Mo and Burkholder, 2010). The same study also suggested full length YneA is the active form, and that the transmembrane domain alone is not sufficient for activity (Mo and Burkholder, 2010). Although YneA is clearly involved in cell division inhibition, the role of this checkpoint in ensuring that daughter cells each receive an intact copy of the genome has not yet been firmly established, and the mechanism by which YneA enforces the checkpoint is still unknown.

The mechanism of relieving the DNA damage checkpoint has only been identified in two bacterial species, *E. coli* and *B. subtilis*. Despite the checkpoint mechanisms functioning in different cellular compartments, the strategy for checkpoint recovery is remarkably similar between these two organisms. In *E. coli*, Lon protease is the major protease responsible for degrading SulA (Mizusawa and Gottesman, 1983; Canceill *et al.*, 1990; Sonezaki *et al.*, 1995), and the protease ClpYQ appears to play a secondary role (Kanemori *et al.*, 1999; Seong *et al.*, 1999; Wu *et al.*, 1999). In *B. subtilis*, there are two proteases YlbL,

which we rename here to DdcP (DNA damage checkpoint recovery protease) and CtpA that degrade YneA (Burby *et al.*, 2018). In the case of DdcP and CtpA, the former seems to be the primary protease in minimal media, however, during chronic exposure to DNA damage in rich media both proteases are important and they can functionally replace each other when overexpressed (Burby *et al.*, 2018). DdcP and CtpA are not regulated by DNA damage (Burby *et al.*, 2018), suggesting that the proteases act as a buffer to YneA accumulation helping to set the threshold for checkpoint activation. Thus, in order for the checkpoint to be enforced both proteases must be saturated. Following repair of damaged DNA, LexA represses expression of YneA and the remaining YneA is cleared by DdcP and CtpA allowing cell division to proceed (Burby *et al.*, 2018).

Although the DNA damage checkpoint in bacteria is well understood, it is becoming increasingly clear that establishing the checkpoint is more complex than what earlier models suggest. Work from Goranov and co-workers demonstrated that the initiation protein and transcription factor DnaA regulates *ftsL* levels in response to DNA replication perturbations, which contributes to cell filamentation (Goranov *et al.*, 2005). Further, our recent report identified several genes not previously implicated in genome maintenance or cell cycle control that are critical for surviving chronic exposure to a broad spectrum of DNA damage (Burby *et al.*, 2018). We identified genes involved in cell division and cell wall synthesis as well as genes of unknown function that rendered the deletion mutants sensitive to DNA damage (Burby *et al.*, 2018). To understand how the DNA damage response in bacteria is regulated, we investigated the contribution of one of the unstudied genes *ddcA* (formerly *ysoA*, see below) in the

DNA damage response. We report here, that DdcA antagonizes YneA action functioning to help set a threshold of DNA damage required for checkpoint activation.

Results

### Deletion of ddcA (ysoA) results in sensitivity to DNA damage

We recently published a set of genome wide screens using three distinct classes of DNA damaging agents, uncovering many genes that have not been previously implicated in the DNA damage response or DNA repair (Burby *et al.*, 2018). One gene that conferred a sensitive phenotype to all three types of DNA damage tested was *ysoA*, which we rename here to DNA damage checkpoint antagonist (*ddcA*). DdcA is a protein that is predicted to have three tetratrichopeptide repeats (Fig. 1A), which are often involved in protein-protein interactions, protein complex formation and virulence mechanisms in bacteria (Cerveny *et al.*, 2013). In order to better understand the mechanism of the DNA damage response in *B. subtilis*, we investigated the contribution of DdcA. To begin, we tested the sensitivity of the *ddcA* deletion to DNA damage. Deletion of *ddcA* resulted in sensitivity to mitomycin C (MMC) an agent that causes DNA crosslinks and bulky adducts; (Iyer and Szybalski, 1963; Noll *et al.*, 2006) and phleomycin a peptide that forms double- and single-strand DNA breaks (Reiter *et al.*, 1972; Kross *et al.*, 1982). We found that expression of P_{xyl}-*ddcA* from an ectopic locus (*amyE*) was sufficient to complement deletion of *ddcA* with or without inducing expression using xylose (Fig. 1B). We conclude that deletion of *ddcA* results in a *bona fide* sensitivity to DNA damage.

DNA damage sensitivity of ddcA deletion is dependent on yneA

We asked how DdcA functions in the DNA damage response. Our observation that a *ddcA* deletion allele results in sensitivity to several DNA damaging agents is similar to the result of deleting the checkpoint recovery proteases (Burby *et al.*, 2018). Our prior study (Burby *et al.*, 2018) showed that DNA damage phenotypes in checkpoint recovery protease mutants depend on the checkpoint enforcement protein, YneA, which is likely the result of aberrant activation of the checkpoint in the absence of YneA degradation. We asked whether deletion of *yneA* could rescue the DNA damage sensitivity resulting from *ddcA* deletion. Indeed, deletion of *yneA* in the *ddcA* deletion background rescued sensitivity to MMC (Fig. S1 and Fig. 2B).

We also tested for a genetic interaction with nucleotide excision repair, reasoning that the absence of nucleotide excision repair would result in increased *yneA* expression and increased sensitivity in the *ddcA* deletion. Indeed,
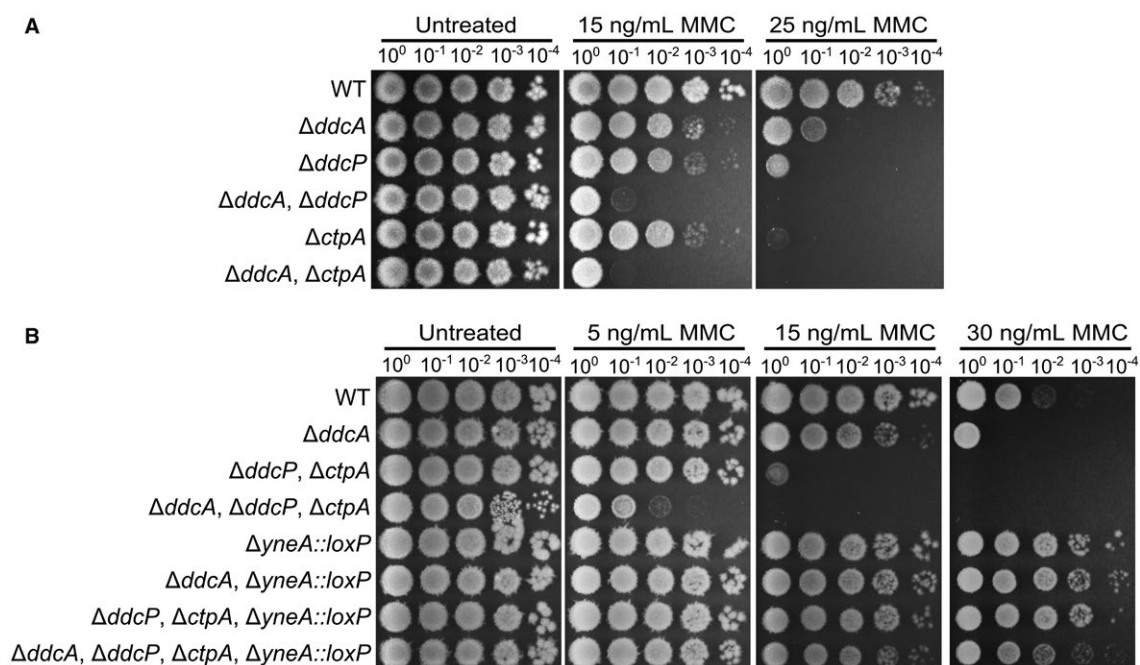
Fig. 2. DdcA functions independent of the checkpoint recovery proteases.
A. Spot titer assay using *B. subtilis* strains WT (PY79), Δ*ddcA* (PEB357), Δ*ddcP* (PEB324), Δ*ddcA* Δ*ddcP* (PEB499), Δ*ctpA* (PEB355) and Δ*ddcA* Δ*ctpA* (PEB579) spotted on the indicated media.
B. Spot titer assay using *B. subtilis* strains WT (PY79), Δ*ddcA* (PEB357), Δ*ddcP* Δ*ctpA* (PEB555), Δ*ddcA* Δ*ddcP* Δ*ctpA* (PEB639), Δ*yneA*::*loxP* (PEB439), Δ*ddcA* Δ*yneA*::*loxP* (PEB587), Δ*ddcP* Δ*ctpA* Δ*yneA*::*loxP* (PEB561) and Δ*ddcA* Δ*ddcP* Δ*ctpA* Δ*yneA*::*loxP* (PEB643) spotted on the indicated media.
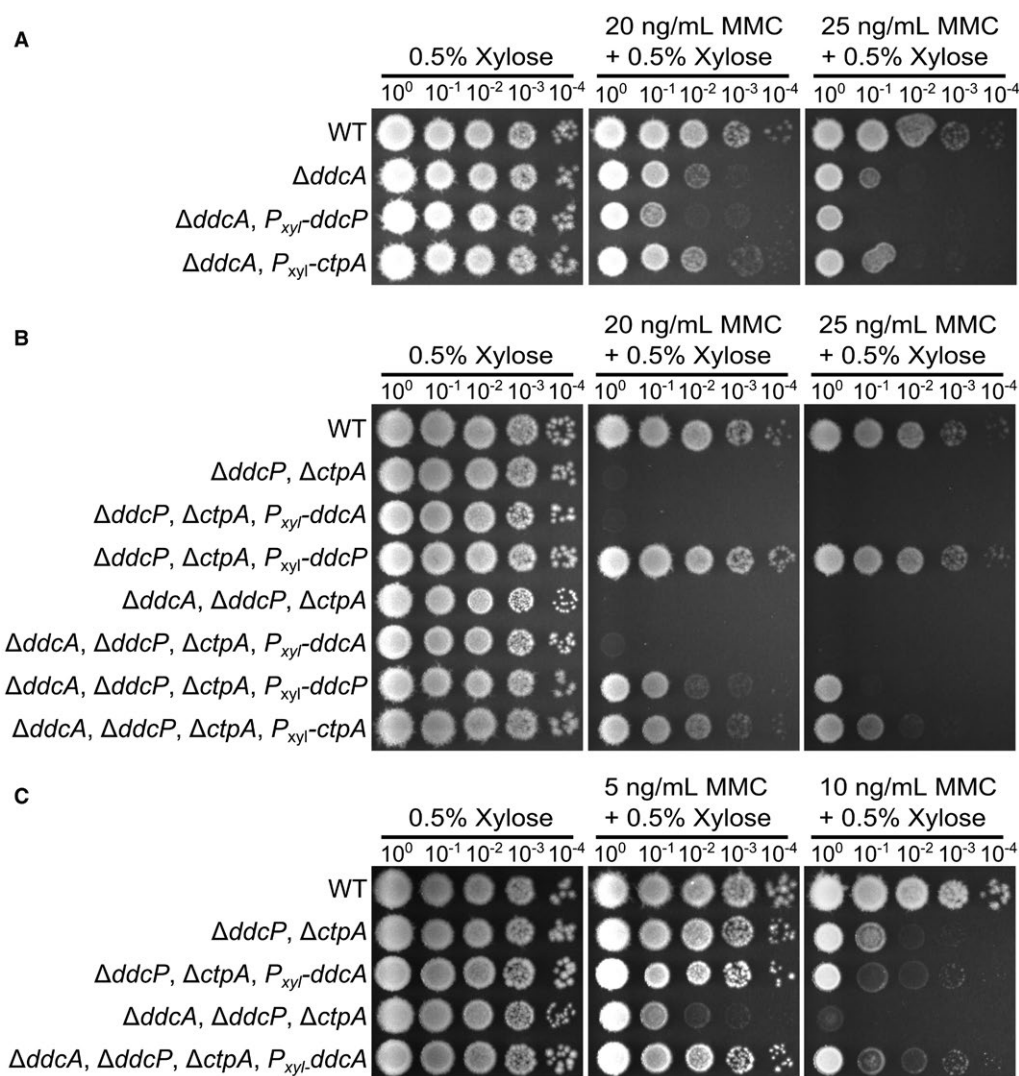
Fig. 3. DdcA cannot complement loss of the checkpoint recovery proteases.
A. Spot titer assay using *B. subtilis* strains WT (PY79), Δ*ddcA* (PEB357), Δ*ddcA amyE*::P_{xyl}-*ddcP* (PEB836) and Δ*ddcA amyE*::P_{xyl}-*ctpA* (PEB837) spotted on the indicated media.
B. Spot titer assay using *B. subtilis* strains WT (PY79), Δ*ddcP* Δ*ctpA* (PEB555), Δ*ddcP*, Δ*ctpA*, *amyE*::P_{xyl}-*ddcA* (PEB838), Δ*ddcP*, Δ*ctpA*, *amyE*::P_{xyl}-*ddcP* (PEB557), Δ*ddcA* Δ*ddcP* Δ*ctpA* (PEB639), Δ*ddcP*, Δ*ctpA*, Δ*ddcA*, *amyE*::P_{xyl}-*ddcA* (PEB840), Δ*ddcP*, Δ*ctpA*, Δ*ddcA*, *amyE*::P_{xyl}-*ddcP* (PEB839), and Δ*ddcP*, Δ*ctpA*, Δ*ddcA and amyE*::P_{xyl}-*ctpA* (PEB841) spotted on the indicated media.
C. Spot titer assay using *B. subtilis* strains WT (PY79), Δ*ddcP* Δ*ctpA* (PEB555), Δ*ddcP*, Δ*ctpA*, *amyE*::P_{xyl}-*ddcA* (PEB838), Δ*ddcA* Δ*ddcP* Δ*ctpA* (PEB639), Δ*ddcP*, Δ*ctpA* and Δ*ddcA*, *amyE*::P_{xyl}-*ddcA* (PEB840) spotted on the indicated media.

deletion of *uvrAB*, genes coding for components of nucleotide excision repair (Sancar, 1996), resulted in hypersensitivity to MMC (Fig. S1). These data, together with the initial observation of general DNA damage sensitivity, and suppression of the sensitivity with loss of *yneA* function suggests that DdcA participates in regulating the DNA damage checkpoint protein YneA.

*DdcA functions independent of the DNA damage checkpoint recovery proteases*

Based on the observation that sensitivity to DNA damage in a Δ*ddcA* mutant was rescued by deletion of *yneA*,

similar to our observations with the checkpoint recovery proteases (Burby *et al.*, 2018), we hypothesized that DdcA could function within the checkpoint recovery process. For example, DdcA could affect CtpA and/or DdcP activity. To test this idea, we generated double mutant strains of Δ*ddcA* with Δ*ctpA* or Δ*ddcP*. If DdcA functions together with CtpA or DdcP, we would expect that the double mutant would have the same phenotype as the single mutant. In contrast, we observed that deletion of *ddcA* in a *ctpA* or *ddcP* mutant resulted in increased sensitivity to MMC (Fig. 2A). These results support the hypothesis that DdcA does not function with the proteases in checkpoint

recovery. To test this idea further, we determined the effect of deletion of *ddcA* in a Δ*ddcP*, Δ*ctpA* double mutant on MMC sensitivity. We found that deletion of *ddcA* resulted in increased MMC sensitivity relative to the double protease mutants (Fig. 2B), suggesting that DdcA functions independently of both DdcP and CtpA. We then asked if *yneA* was responsible for the phenotype of Δ*ddcA* in the absence of the checkpoint recovery proteases. Strikingly, we found that the sensitivity of the triple mutant was mostly dependent on *yneA*, but at elevated concentrations of MMC, there was a slight but reproducible difference when *ddcA* was deleted in the Δ*ddcP, ΔctpA, ΔyneA*::*loxP* mutant background (Fig. 2B). Taken together, these data suggest that DdcA regulation of the checkpoint is independent of the recovery proteases. Further, because the *ddcA* phenotype is dependent on *yneA* we suggest that DdcA negatively regulates the checkpoint enforcement protein YneA.

In our previous study, we found that the checkpoint recovery proteases could substitute for each other (Burby *et al.*, 2018). Therefore, to more firmly establish when DdcA regulates the checkpoint we asked if DdcA could replace the checkpoint recovery proteases or if the proteases could function in place of DdcA. To test this idea, we overexpressed *ddcP* and *ctpA* in a Δ*ddcA* mutant and

found that neither protease could rescue a *ddcA* deletion phenotype (Fig. 3A). We also found that expression of *ddcA* in the double protease mutant could not rescue the MMC-sensitive phenotype (Fig. 3B). Further, expression of *ddcP* or *ctpA* were each able to partially complement the phenotype of the triple mutant, but expression of *ddcA* had no effect at higher concentrations of MMC (Fig. 3B). As a control, we verified that overexpression of *ddcA* using high levels of xylose (0.5% xylose) could complement a Δ*ddcA* mutant (Fig. S2). We also found that at lower concentrations of MMC, expression of *ddcA* could rescue the *ddcA* deficiency of the triple mutant resulting in a phenotype indistinguishable from the double protease mutant (Fig. 3C). Given that DdcA cannot substitute for DdcP and CtpA, we hypothesized that DdcA would not affect YneA protein levels following DNA damage. We tested this by monitoring YneA protein levels following MMC treatment and after recovering from MMC treatment for 2 h. Deletion of *ddcA* alone did not result in a detectable difference in YneA protein levels compared to WT (Fig. S3). Further, deletion of *ddcA* in the double protease mutant also did not result in an increase in YneA protein levels relative to the double protease mutant with *ddcA* intact (Fig. S3). With these data, we conclude that DdcA does not regulate YneA protein abundance.
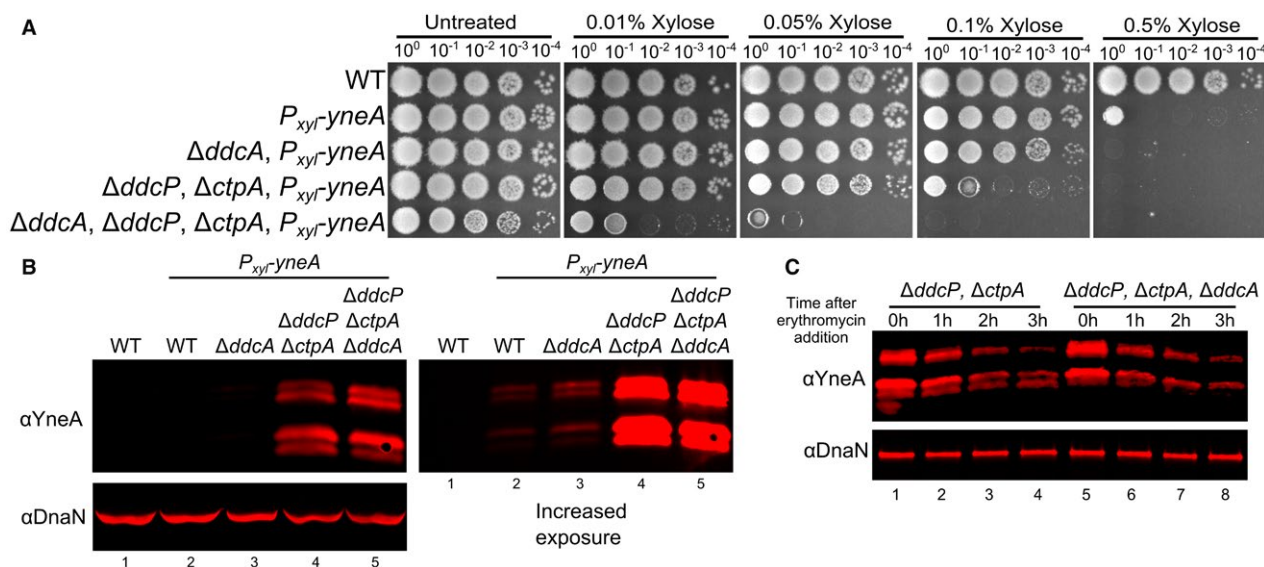

Fig. 4. Deletion of *ddcA* results in sensitivity to *yneA* overexpression independent of YneA stability.
A. Spot titer testing the effect of *yneA* overexpression. *B. subtilis* strains WT (PY79), *amyE*::P$_{xyl}$-*yneA* (PEB846), Δ*ddcA amyE*::P$_{xyl}$-*yneA* (PEB848), Δ*ddcP*, Δ*ctpA, amyE*::P$_{xyl}$-*yneA* (PEB850) and Δ*ddcA* Δ*ddcP* Δ*ctpA, amyE*::P$_{xyl}$-*yneA* (PEB852) were spotted on LB agar media containing increasing concentrations of xylose to induce *yneA* expression.
B. A Western blot using antisera against YneA (Upper panels), or DnaN lower panel using *B. subtilis* strains WT (PY79), *amyE*::P$_{xyl}$-*yneA* (PEB846), Δ*ddcA amyE*::P$_{xyl}$-*yneA* (PEB848), Δ*ddcP*, Δ*ctpA, amyE*::P$_{xyl}$-*yneA* (PEB850) and Δ*ddcA* Δ*ddcP* Δ*ctpA, amyE*::P$_{xyl}$-*yneA* (PEB852) after growing in the presence of 0.1% xylose for 2 h. The panel on the right is an increased exposure to show the faint bands of WT and Δ*ddcA*.
C. A Western blot using antisera against YneA (upper panel) or DnaN (lower panel). Cultures of Δ*ddcP*, Δ*ctpA, amyE*::P$_{xyl}$-*yneA* (PEB850) and Δ*ddcA* Δ*ddcP* Δ*ctpA and amyE*::P$_{xyl}$-*yneA* (PEB852) were grown as in panel B, except at 0 h erythromycin was added and samples were harvest every hour for 3 h. [Colour figure can be viewed at wileyonlinelibrary.com]
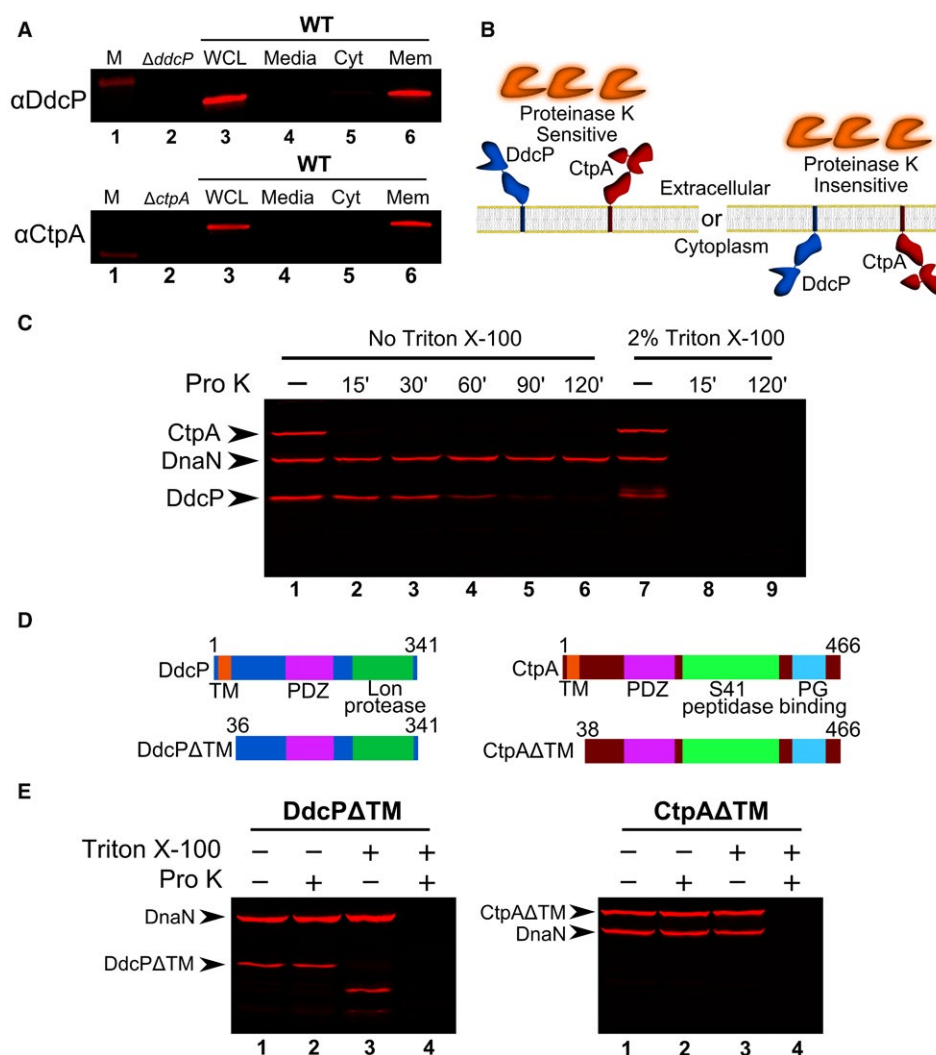
Fig. 5. DdcP and CtpA are membrane anchored with extracellular protease domains.
A. Subcellular fractionation followed by Western blot analysis of WT (PY79) lysates using DdcP and CtpA antisera (M, molecular weight standard, WCL, whole cell lysates; Media, precipitated media proteins; Cyt, cytosolic fraction; Mem, membrane fraction).
B. Competing models for membrane topology of DdcP and CtpA tested using a proteinase K sensitivity assay.
C. Proteinase K sensitivity assay followed by Western blot detection of DdcP, CtpA and DnaN with antiserum. Samples were treated with lysozyme to generate protoplasts and incubated with proteinase K for the indicated time (lanes 1-6), or the samples were incubated with lysozyme and Triton X-100 to disrupt the plasma membrane and incubated with proteinase K for the indicated time (lanes 7-9).
D. Schematics depicting the DdcPΔTM (left) and CtpAΔTM (right) in which the transmembrane domain was deleted.
E. Proteinase K sensitivity assay followed by Western blot analysis of strains expressing DdcPΔTM (left, PEB719) or CtpAΔTM (right, PEB772) performed as in panel C using a 2 h incubation with proteinase K. [Colour figure can be viewed at wileyonlinelibrary.com]

ddcA deletion results in sensitivity to yneA overexpression independent of YneA stability

Prior work established that overexpression of *yneA* resulted in growth inhibition (Kawai *et al.*, 2003; Mo and Burkholder, 2010). Previously, we demonstrated that the double checkpoint recovery protease mutant was considerably more sensitive than the WT strain or the single checkpoint protease mutants to *yneA* overexpression (Burby *et al.*, 2018). Given that treatment with DNA damage has cellular consequences in addition to expression of *yneA*, we wanted to test whether overexpression of

yneA was sufficient for enhanced growth inhibition in the absence of *ddcA*. Indeed, we found that the Δ*ddcA* mutant was more sensitive to *yneA* overexpression than WT (Fig. 4A), and that deletion of *ddcA* in the double protease mutant background resulted in even greater sensitivity to *yneA* overexpression than the double mutant or each single mutant (Fig. 4A, (Burby *et al.*, 2018)). Therefore, we asked whether YneA protein levels changed under these conditions, and again there was no detectable difference when *ddcA* was deleted alone or in combination with the double protease mutant (Fig. 4B). We also considered

the possibility that DdcA could affect the stability of YneA rather than the overall amount. To test this idea, we performed a translation shut-off experiment and monitored YneA stability over time. We induced expression of *yneA* in the double protease mutant with and without *ddcA* and blocked translation. We found that YneA protein abundance decreased at a similar rate regardless of whether *ddcA* was present (Fig. 4C). We conclude that DdcA negatively regulates YneA independent of protein stability.
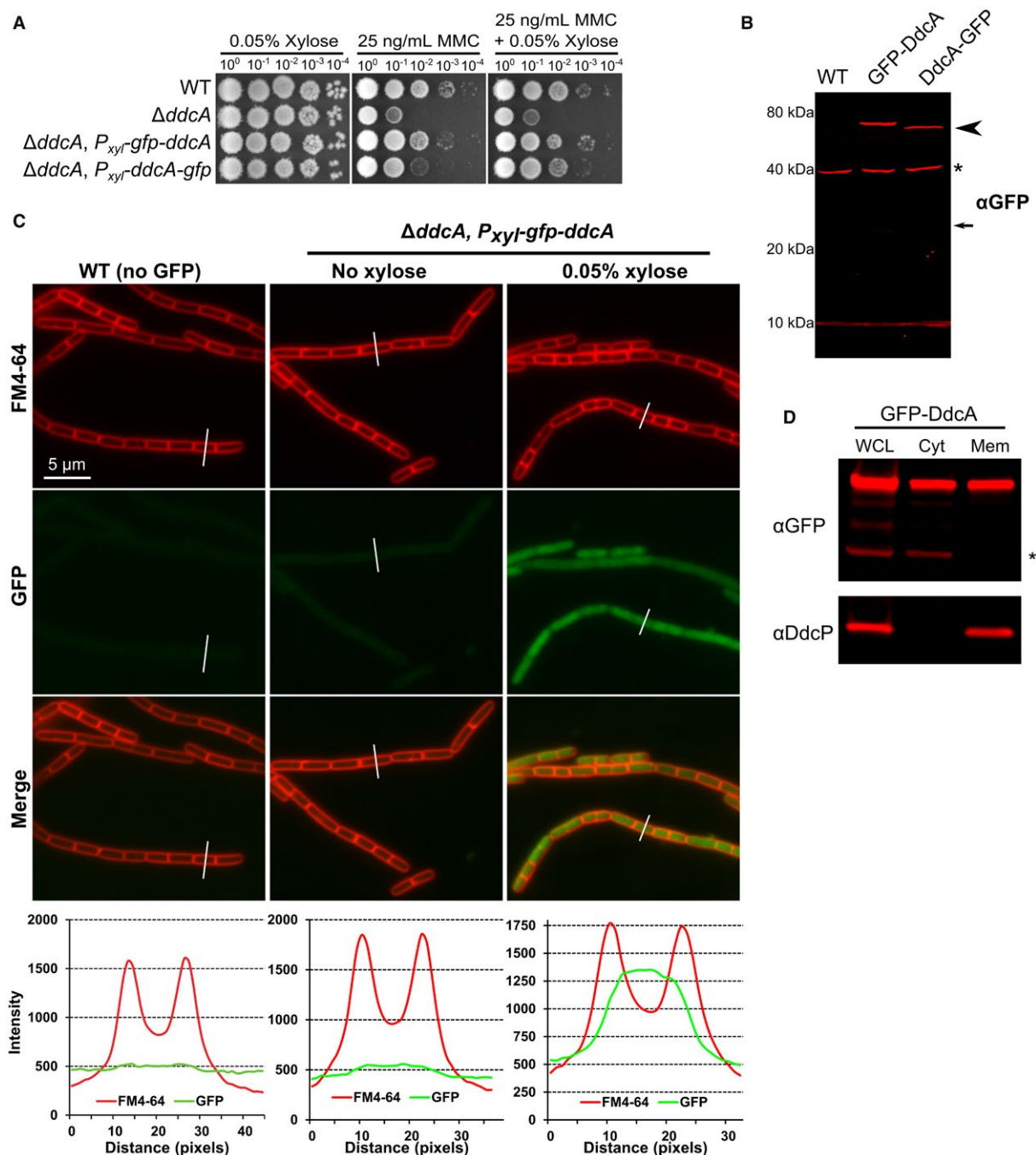
DdcA is an intracellular protein and DdcP and CtpA are membrane anchored with extracellular protease domains

The observation that DdcA and the checkpoint recovery proteases have distinct functions led us to ask where these proteins are located within the cell to determine if there are spatial constraints on their regulation of the DNA damage checkpoint. YneA is a membrane protein with the majority of the protein located extracellularly (Mo and Burkholder, 2010). We hypothesized that proteases DdcP and CtpA should be similarly localized since YneA is a direct substrate (Burby *et al.*, 2018). We used the transmembrane prediction software TMHMM (Krogh *et al.*, 2001) and found that both DdcP and CtpA were predicted to have an N-terminal transmembrane domain, as reported previously (Tjalsma *et al.*, 2000). We tested this prediction directly using a subcellular fractionation assay (Wu and Errington, 1997). We found that DdcP and CtpA were present predominantly in the membrane fraction (Fig. 5A). DdcP is predicted to have a signal peptide cleavage site (Tjalsma *et al.*, 2000); however, we did not detect DdcP in the media (Fig. 5A), suggesting that DdcP is membrane anchored and not secreted. The membrane topology of DdcP and CtpA could put the protease domains inside or outside of the cell (Fig. 5B). To determine their location, we used a protease sensitivity assay (Fig. 5B; Wilson *et al.*, 2012). Cells were treated with lysozyme, followed by incubation with proteinase K. We found that DdcP and CtpA were digested by proteinase K, but that the intracellular protein DnaN was not (Fig. 5C). In control reactions, we added Triton X-100 to disrupt the plasma membrane, which rendered all three proteins susceptible to proteinase K (Fig. 5C). To verify that the N-terminal transmembrane domain is required for DdcP and CtpA to be extracellular we created N-terminal truncations (Fig. 5D), and repeated the proteinase K sensitivity assay. With these variants, DdcP and CtpA should be locked inside the cell, and indeed, both N-terminal truncations were now resistant to proteinase K similar to DnaN (Fig. 5E). We conclude that DdcP and CtpA are tethered to the plasma membrane through N-terminal transmembrane domains and their protease domains are extracellular (Fig. 5B, left panel).

YneA has a transmembrane domain and has previously been shown to be localized to the plasma membrane (Mo and Burkholder, 2010), and we now show that DdcP and CtpA are membrane anchored as well. To better understand how DdcA limits YneA activity, we asked where DdcA is located. We were unable to find DdcA detected in any previous proteomic experiments that interrogated cytosolic or extracellular proteins (Hirose *et al.*, 2000; Buttner *et al.*, 2001; Eymann *et al.*, 2004). Also, the secretome of *B. subtilis* was analyzed using bioinformatics and did not report DdcA as a secreted protein (Tjalsma *et al.*, 2000). Therefore, we used several programs to predict the subcellular location of DdcA (Hofmann and Stoffel, 1993; Krogh *et al.*, 2001; Bendtsen *et al.*, 2005; Yu *et al.*, 2010), all of which suggested that DdcA is cytosolic.

In order to experimentally determine the location of DdcA, we generated GFP fusions to the N- and C-termini of DdcA. We tested whether GFP-DdcA and DdcA-GFP were functional by assaying for the ability to complement a *ddcA* deletion. We found that GFP-DdcA was able to complement a *ddcA* deletion in the presence or absence of xylose for induced expression (Fig. 6A), similar to that observed with untagged DdcA (Fig. 1). In contrast, DdcA-GFP was partially functional, because complete complementation was only observed when expression of *ddcA-gfp* was induced using xylose, but not in the absence of xylose (Fig. 6A). As a control we asked if we could detect free GFP via western blotting using GFP-specific antiserum. We did not detect the fusion proteins in lysates if expression was not induced using xylose. We found that both DdcA fusions were detectable at their approximate molecular weight of 67.6 kDa when induced with 0.05% xylose (Fig. 6B), though we did see that the C-terminal fusion had a slight increase in mobility (Fig. 6B, arrowhead). Importantly, we did not detect a significant band near 25 kDa, the approximate size of GFP (Fig. 6B), suggesting that GFP is not cleaved from DdcA. We did detect a very faint proteolytic fragment (Fig. 6B, arrow) that seemed to occur during the lysis procedure. After establishing the functionality and integrity of the GFP-DdcA fusion, we chose to visualize DdcA localization via fluorescence microscopy.

To compare the background fluorescence of *B. subtilis* cells, we imaged WT (PY79) cells under the same conditions as the GFP-DdcA fusion strain. We found a low level of background fluorescence in WT cells, and when a line scan of fluorescence intensity through a cell was plotted there was a very slight increase in signal intensity in the span between the fluorescent membrane peaks (Fig. 6C). The GFP-DdcA fusion was detectable throughout the cell at very low levels in the absence of xylose induction, with the intensity being slightly greater than WT cells (Fig. 6C). We then imaged cells under conditions in which *gfp-ddcA* expression was induced with 0.05% xylose. This experiment shows that GFP-DdcA

Fig. 6. GFP-DdcA is an intracellular protein and is present in the cytosolic and membrane fractions.
A. Spot titer assay using *B. subtilis* strains WT (PY79), Δ*ddcA* (PEB357), Δ*ddcA amyE*::P_{xyl}-*gfp-ddcA* (PEB854) and Δ*ddcA amyE*::P_{xyl}-*ddcA-gfp* (PEB856) spotted on the indicated media.
B. Western blot of cell extracts from *B. subtilis* strains WT (PY79), Δ*ddcA amyE*::P_{xyl}-*gfp-ddcA* (PEB854) and Δ*ddcA amyE*::P_{xyl}-*ddcA-gfp* (PEB856) using antiserum against GFP. The arrowhead highlights the slightly increased mobility of DdcA-GFP, and the asterisk denotes a cross-reacting species detected by the GFP antiserum. The smaller arrow indicates the expected migration of free GFP.
C. Micrographs from WT (PY79) and Δ*ddcA amyE*::P_{xyl}-*gfp-ddcA* (PEB854) cultures grown in S7$_{50}$ minimal media containing 1% arabinose with (far left and right panels) or without (middle panels) 0.05% xylose. Images in red are the membrane stain FM4-64, green are GFP fluorescence and the bottom images are a merge of FM4-64 and GFP fluorescence. The white lines through cells in the images are a representation of the line scans of fluorescence intensity generated in ImageJ and plotted below the micrographs. Scale bar is 5 μm.
D. Western blot of whole cell lysate (WCL), cytosolic fraction (Cyt), and membrane fraction (Mem) from Δ*ddcA amyE*::P_{xyl}-*gfp-ddcA* (PEB854) cell extracts using antisera against GFP (upper panel) or DdcP (lower panel). The asterisk denotes a cross-reacting species detected by the GFP antiserum. [Colour figure can be viewed at wileyonlinelibrary.com]
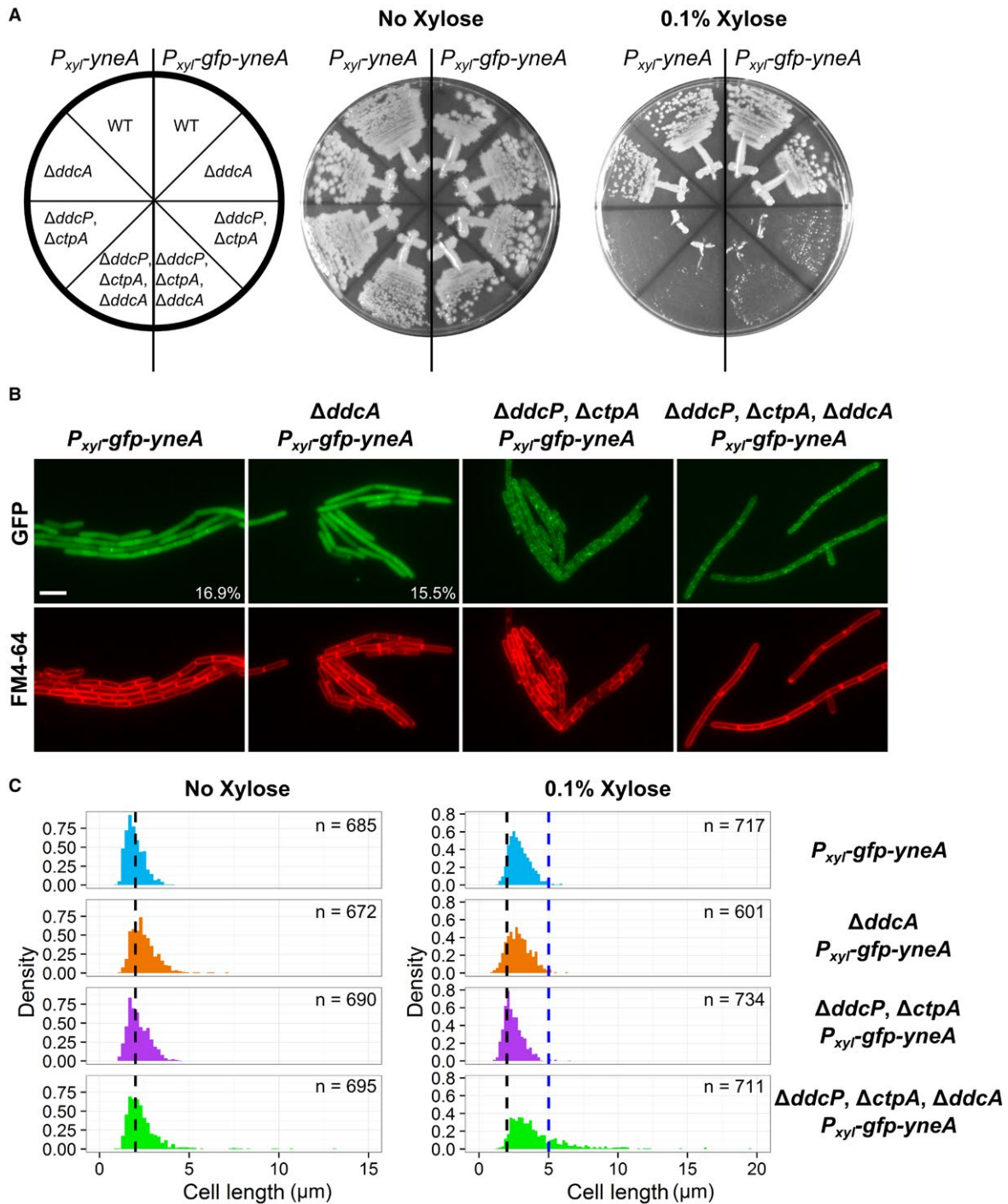
Fig. 7. DdcA inhibits YneA.

A. *B. subtilis* strains *amyE*::P_{xyl}-*yneA* (PEB846), Δ*ddcA amyE*::P_{xyl}-*yneA* (PEB848), Δ*ddcP*, Δ*ctpA*, *amyE*::P_{xyl}-*yneA* (PEB850) and Δ*ddcA* Δ*ddcP* Δ*ctpA*, *amyE*::P_{xyl}-*yneA* (PEB852), *amyE*::P_{xyl}-*gfp-yneA* (PEB876), Δ*ddcA amyE*::P_{xyl}-*gfp-yneA* (PEB882), Δ*ddcP*, Δ*ctpA*, *amyE*::P_{xyl}-*gfp-yneA* (PEB888) and Δ*ddcA* Δ*ddcP* Δ*ctpA*, *amyE*::P_{xyl}-*gfp-yneA* (PEB894) were struck onto LB or LB + 0.1% xylose and incubated at 30°C overnight. The scale bar is 5 μm.

B. Micrographs from the indicated strains from Panel A, grown in minimal media and treated with 0.1% xylose for 30 min. Green images are GFP fluorescence and red images are FM4-64 membrane stain. The percentage of septal localization is shown for PEB876 (n = 591) and PEB882 (n = 542). The p-value of a two-tailed z-test was 0.516.

C. Cell length distributions of strains grown with (right) or without (left) 0.1% xylose. The number of cells measured (n) for each condition is indicated. The black dashed line is drawn at 2 μm. [Colour figure can be viewed at wileyonlinelibrary.com]

was found throughout the cytosol, and the scan of fluorescence intensity was significantly greater than WT (Fig. 6C). We observed that the partially functional DdcA-GFP fusion was also present diffusely throughout the cytosol (Fig. S3A). Finally, we tested DdcA localization using subcellular fractionation. We found that GFP-DdcA was detectable in the membrane and cytosolic fractions (Fig. 6D), and similar results were obtained with DdcA-GFP (Fig. S4B). As controls, we found that DdcP was found in the membrane fraction and not the cytosolic fraction (Fig. 6D), and a cross-reacting protein detected by our GFP antiserum was found in the cytosol and not the membrane fractions (Fig. 6D). Taken together, DdcA appears to be an intracellular protein that is primarily located in the cytosol with some molecules localized to the membrane. Importantly, we now show that DdcA and the checkpoint recovery proteases are separated in space by the plasma membrane, demonstrating that YneA regulators are present in the cytosol (DdcA) and in the extracellular space (DdcP and CtpA). Further, the demonstration of DdcA occupying a different subcellular location from DdcP and CtpA explains their distinct roles in regulating YneA.

YneA-dependent cell elongation is enhanced in cells lacking DdcA and the recovery proteases

DdcA appears to regulate YneA activity independent of protein abundance and stability. We initially hypothesized that DdcA could interact directly with YneA to inhibit its activity. To test this hypothesis, we assayed for a protein-protein interaction using a bacterial two-hybrid, but did not detect an interaction (Fig. S5). We then asked whether DdcA affected the localization of YneA, hypothesizing that DdcA could prevent YneA from reaching the plasma membrane. To address this question, we built a strain in which GFP was fused to the N-terminus of YneA, and placed *gfp-yneA* under the control of the xylose-inducible promoter P_{xyl}. We expressed both YneA and GFP-YneA in strains lacking *ddcA*, the checkpoint recovery proteases, or the triple mutant and found that GFP-YneA is able to inhibit growth to a similar extent as YneA (Fig. 7A), suggesting that the GFP fusion is functional. We visualized GFP-YneA following induction with 0.1% xylose for 30 min. We found that GFP-YneA localized to the mid-cell while also demonstrating diffuse intracellular fluorescence (Fig. 7B), which we suggest is free GFP generated by the checkpoint recovery proteases after YneA cleavage. Deletion of *ddcA* alone did not affect GFP-YneA localization, with both WT and Δ*ddcA* strains having similar mid-cell localization frequencies (Fig. 7B). The absence of both checkpoint recovery proteases resulted in puncta throughout the plasma membrane (Fig. 7B).

Intriguingly, deletion of *ddcA* in addition to the checkpoint recovery proteases resulted in severe cell elongation, however, GFP-YneA localization was not affected (Fig. 7B). The difference in cell length was quantified by measuring the cell length of at least 600 cells following growth in the presence of 0.1% xylose for 30 min. The cell length distributions of strains lacking *ddcA* or *ddcP* and *ctpA* were similar to the WT control (Fig. 7C). The distribution for the strain lacking *ddcA*, *ddcP* and *ctpA* had a significant skew to the right indicating greater cell lengths (Fig. 7C). The percentage of cells greater than 5 μm in length was approximately 22% for the triple mutant and significantly greater than the other three strains in which approximately 1% of cells were greater than 5 μm (Table 1). As a control, we determined the cell length distributions prior to xylose addition and found all four strains to have similar cell length distributions in the absence of xylose (Fig. 7C). With these data, we conclude that DdcA prevents YneA from inhibiting cell division.

Table 1. Overexpression of GFP-YneA results in a significant increase in cells greater than 5 μm for cells lacking *ddcP*, *ctpA* and *ddcA*.

Strain	Genotype	No Xylose	0.1% Xylose		
		Cell length (mean ± sd)	Cell length (mean ± sd)	% ≥ 5 μm	p-value
PEB876	*amyE*::P_{xyl}-*gfp-yneA*	1.98 ± 0.51 (n = 685)	2.91 ± 0.75	0.84% (6/717)	N/A
PEB882	Δ*ddcA*, *amyE*::P_{xyl}-*gfp-yneA*	2.48 ± 0.73 (n = 672)	2.86 ± 0.85	1.16% (7/601)	0.55
PEB888	Δ*ddcP*, Δ*ctpA*, *amyE*::P_{xyl}-*gfp-yneA*	2.18 ± 0.60 (n = 690)	2.49 ± 0.70	0.68% (5/734)	0.73
PEB894	Δ*ddcP*, Δ*ctpA*, Δ*ddcA*, *amyE*::P_{xyl}-*gfp-yneA*	2.39 ± 1.10 (n = 695)	4.09 ± 2.09	22.4% (159/711)	<0.00001

Data are from expression of GFP-YneA using 0.1% xylose for 30 min. The mean cell length ± the standard deviation is listed. The percent of cells greater than 5 μm (number/total cells scored) and the p-value from a two-tailed z-test are listed.

Discussion

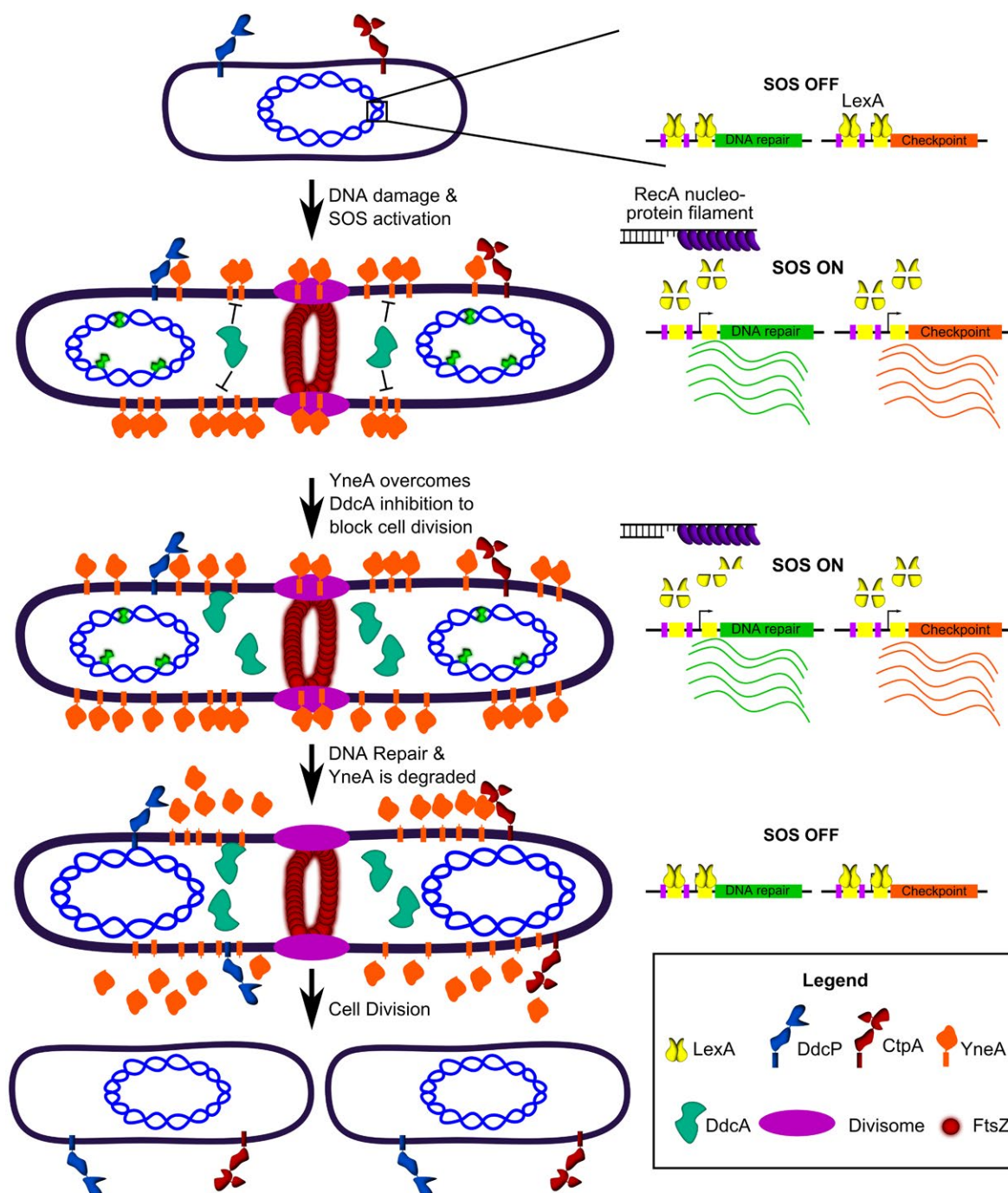*A model for DNA damage checkpoint activation and recovery*

The DNA damage checkpoint in bacteria was discovered through seminal work using *E. coli* as a model organism (Friedberg *et al.*, 2006). An underlying assumption in the models is that the input signal of RecA-coated ssDNA and the affinity of LexA for its binding site is sufficient to control the rate of cell division in response to DNA damage. A finding that the initiator protein, DnaA, controls the transcription of *ftsL*, and as a result the rate of cell division, in response to replication stress, gave a hint that coordination of cell division and DNA replication may be more complex (Goranov *et al.*, 2005). Here, we elaborate on the complexity of regulating cell division in response to DNA damage by uncovering a DNA damage checkpoint antagonist, DdcA (Fig. 8). In response to DNA damage, the repressor LexA is inactivated, which results in expression of *yneA*. Accumulation of YneA must saturate two proteases, DdcP and CtpA, and overcome DdcA-dependent inhibition in order to block cell division. We previously reported that DdcP and CtpA are not induced by DNA damage (Burby *et al.*, 2018), and a previous study reported that transcripts of *ddcA*, *ddcP* and *ctpA* are not induced by DNA damage or inhibition of DNA replication (Goranov *et al.*, 2006). Thus, we model all three proteins functioning to set a threshold of YneA required for checkpoint activation with DdcA located in the cytosol and DdcP and CtpA protease domains located extracellularly. These regulators require that YneA expression overcomes a cytosolic regulator and then two extracellular regulators before the checkpoint can be activated. After the checkpoint is established, DNA repair occurs and the integrity of the DNA is restored, the SOS response is turned off, LexA represses *yneA* expression and the checkpoint recovery proteases degrade the remaining YneA. The genetic experiments attempting to substitute the checkpoint proteases for DdcA and vice versa strongly suggest that DdcA does not function in the checkpoint recovery process (Fig. 3). Together, our results uncover a unique strategy in regulating a bacterial DNA damage checkpoint by identifying a proteolysis independent mechanism of setting a threshold for DNA damage checkpoint activation.

How does DdcA inhibit YneA?

Our results are most supportive of DdcA acting as an antagonist to YneA, rather than functioning in checkpoint recovery. Two lines of evidence support this model. First, DdcA does not affect YneA protein levels, stability or localization (Figs S3 and S4). Second, if DdcA was involved in checkpoint recovery, we would predict that

expression of one of the checkpoint proteases would be able to compensate for deletion of *ddcA*. Instead, we found that the checkpoint recovery proteases and DdcA cannot replace each other (Fig. 3). As a result, we hypothesized that DdcA acts by preventing YneA from accessing its target. We tested for an interaction between YneA and DdcA using a bacterial two-hybrid assay and we were unable to identify an interaction with full length or a cytoplasmic 'locked' YneA mutant lacking its transmembrane domain (Fig. S5). We also ruled out the hypothesis that DdcA affects the subcellular localization of YneA using a GFP-YneA fusion, which had similar localization patterns with and without *ddcA* (Fig. 7B). Taken together, all these results support a model where DdcA prevents YneA from inhibiting cell division, which could occur through preventing access to the target of YneA or through an indirect mechanism.

The YneA target that results in the inhibition of cell division is unknown. YneA is a membrane bound cell division inhibitor. This class of inhibitor in bacteria is typified as being a small protein that contains an N-terminal transmembrane domain, and they have been identified in several species (Kawai *et al.*, 2003; Chauhan *et al.*, 2006; Ogino *et al.*, 2008; Modell *et al.*, 2011; 2014; Bojer *et al.*, 2018). In *C. crescentus*, the cell division inhibitors SidA and DidA inhibit the activity of FtsW/N, which are components of the divisome. A recent study in *Staphylococcus aureus* identified a small membrane division inhibitor, SosA, and its target appears to be PBP1 (Bojer *et al.*, 2018), which is involved in peptidoglycan synthesis at the septum (Scheffers and Errington, 2004; Claessen *et al.*, 2008). It is tempting to speculate that YneA could target an essential component of the cell division machinery, in particular because previous work found a conserved face of the transmembrane domain that was required for activity (Mo and Burkholder, 2010). Prior studies of *C. crescentus* and *S. aureus* were able to detect interactions between the cell division inhibitors and their targets using the bacterial two-hybrid assay (Modell *et al.*, 2011; 2014; Bojer *et al.*, 2018). We reasoned that we might be able to identify an interacting partner of YneA or DdcA using this approach. We used DdcA and YneA in a bacterial two-hybrid assay using several proteins involved in cell division and cell wall synthesis, many of which had phenotypes in our previous Tn-seq genetic screens (Burby *et al.*, 2018), but we were unable to identify a positive interaction (data not shown). Still, there are fundamental differences between YneA and other membrane bound cell division inhibitors. YneA has two major predicted features: an N-terminal transmembrane domain and a C-terminal LysM domain, and both have been found to be required for full activity (Mo and Burkholder, 2010). The other cell division inhibitors SidA, DidA, and SosA do not have a LysM domain (Modell *et al.*, 2011; 2014; Bojer *et*

Fig. 8. DdcA inhibits enforcement of the DNA damage checkpoint. A working model for how DdcA inhibits YneA. DdcA prevents access to the target of YneA, however, when the SOS response has been activated for a prolonged period of time, YneA is able to overcome DdcA-dependent inhibition to prevent cell division. Following DNA repair and completion of DNA replication the SOS response is turned off and the checkpoint recovery proteases degrade YneA allowing cell division to resume. [Colour figure can be viewed at wileyonlinelibrary.com]

al., 2018). LysM domains bind to peptidoglycan (PG) and many proteins containing LysM domains have cell wall hydrolase activity (Buist *et al.*, 2008). Thus, another possibility is that YneA acts directly on the cell wall to inhibit cell division instead of or in addition to targeting a membrane protein.

Intriguingly, the cell division inhibitor of *Mycobacterium tuberculosis*, Rv2719c, also contains a LysM domain and was shown to have cell wall hydrolase activity *in vitro* (Chauhan *et al.*, 2006). The localization of GFP-YneA is also similar to previous reports of fluorescent vancomycin labeling of nascent peptidoglycan synthesis (Fig.

7B; Daniel and Errington, 2003; Tiyanont *et al.*, 2006). The difficulty with the model of targeting cell wall synthesis directly is that it is not clear how DdcA would prevent YneA activity given that these proteins are separated by the plasma membrane. One explanation is that DdcA directly or indirectly affects the folding of YneA as it is transported across the membrane, resulting in a form of YneA that is not competent for PG binding. DdcA contains a TPR domain and proteins containing TPR domains have been found to have chaperone activity and act as co-chaperones (Smith, 2004). It is intriguing that *ddcA* is just upstream of the chaperone trigger factor (*tig*) in the *B. subtilis* genome, and this organization is conserved in some bacterial species.

Negative regulation of YneA occurs through three distinct mechanisms

The checkpoint recovery proteases and DdcA utilize multiple strategies to inhibit YneA. Although both DdcP and CtpA degrade YneA, they are very different proteases. DdcP has a Lon peptidase domain and a PDZ domain, whereas CtpA has an S41 peptidase domain and a PDZ domain. The PDZ domains of DdcP and CtpA have different functions *in vivo* and show homology to different classes of PDZ domains found in proteases in *E. coli* (Fig. S6, see supporting results). Thus, it appears that the proteases utilize different strategies to degrade YneA. DdcA is unique, because it acts as an antagonist without affecting protein abundance, stability or localization. Also, DdcA appears to function prior to checkpoint establishment and not in recovery, whereas the proteases perform both functions. Together, DdcA, DdcP and CtpA provide a buffer to expression of YneA, thereby setting a threshold of YneA for checkpoint enforcement.

The discovery of a specific DNA damage checkpoint antagonist brings the total known proteins to negatively regulate YneA to three, which begs the question: why isn't a single protein sufficient? One explanation is that the process can be fine-tuned. By utilizing several proteins, the process has more nodes for regulation, which is advantageous at least for *B. subtilis*. A second explanation is that this strategy evolved in response to more efficient DNA repair. The SOS-regulon is highly conserved in bacteria and yet the checkpoint strategies vary significantly (Erill *et al.*, 2007). If an organism evolves a more efficient DNA repair system in which DNA repair could be completed faster, the same level of checkpoint protein will no longer be required, because the checkpoint would delay cell division longer than necessary to complete DNA repair. This could be the explanation for the highly divergent nature of cell division inhibitors in bacteria as well as the explanation for the complex control over YneA found in *B. subtilis*.

Experimental procedures

Bacteriological and molecular methods

All *B. subtilis* strains are derivatives of PY79 (Youngman *et al.*, 1984), and are listed in Table 2. Construction of individual strains is detailed in the supporting methods using double cross-over recombination or CRISPR/Cas9 genome editing as previously described (Burby and Simmons, 2017; Burby *et al.*, 2018). *Bacillus subtilis* strains were grown in LB (10 g/L NaCl, 10 g/L tryptone, 5 g/L yeast extract) or $S7_{50}$ media [1× $S7_{50}$ salts (diluted from 10× $S7_{50}$ salts: 104.7 g/L MOPS, 13.2 g/L, ammonium sulfate, 6.8 g/L monobasic potassium phosphate, pH 7.0 adjusted with potassium hydroxide), 1× metals (diluted from 100× metals: 0.2 M $MgCl_2$, 70 mM $CaCl_2$, 5 mM $MnCl_2$, 0.1 mM $ZnCl_2$, 100 µg/mL thiamine-HCl, 2 mM HCl, 0.5 mM $FeCl_3$), 0.1% potassium glutamate, 40 µg/mL phenylalanine, 40 µg/mL tryptophan] containing either 2% glucose or 1% arabinose as indicated in each method. Plasmids used in this study are listed in Table S1. Individual plasmids were constructed using Gibson assembly as described previously (Gibson, 2011; Burby *et al.*, 2018). The details of plasmid construction are described in the supporting methods. Oligonucleotides used in this study are listed in Table S2 and were obtained from Integrated DNA technologies (IDT). Antibiotics for selection in *B. subtilis* were used at the following concentrations: 100 µg/mL spectinomycin, 5 µg/mL chloramphenicol and 0.5 µg/mL erythromycin. Antibiotics used for selection in *E. coli* were used at the following concentrations: 100 µg/mL spectinomycin, 100 µg/mL ampicillin and 50 µg/mL kanamycin. Mitomycin C (Fisher bioreagents) and phleomycin (Sigma) were used at the concentrations indicated in the figures and legends.

Spot titer assays

Spot titer assays were performed as previously described (Burby *et al.*, 2018). Briefly, *B. subtilis* strains were grown on an LB agar plate at 30°C overnight and a single colony was used to inoculate a liquid LB culture. The cultures were grown at 37°C to an OD_{600} between 0.5 and 1. Cultures were normalized to an $OD_{600} = 0.5$, and serial dilutions were spotted on to LB agar media containing the drugs as indicated in the figures. Plates were grown at 30°C overnight (16-20 h). All spot titer assays were performed at least twice.

Western blotting

Western blotting experiments for YneA were performed essentially as described (Burby *et al.*, 2018). Briefly, for the MMC recovery assay, samples of an $OD_{600} = 10$ were harvested via centrifugation and washed twice with 1× PBS pH 7.4 and re-suspended in 400 µL of sonication buffer (50 mM Tris, pH 8.0, 10 mM EDTA, 20% glycerol, 2× Roche protease inhibitors and 5 mM PMSF) and lysed via sonication. SDS sample buffer was added to 2× and samples (10 µL) were incubated at 100°C and separated using 10% SDS-PAGE (DnaN) or 16.5% Tris-Tricine SDS-PAGE (YneA). Proteins were transferred to a nitrocellulose membrane using the BioRad transblot-turbo following the manufacturer's

Table 2. Strains used in this study.

Strain	Genotype	Reference
PY79	PY79	Youngman *et al.* (1984)
PEB309	$\Delta uvrAB$	This study
PEB324	$\Delta ddcP$ (*ylbL*)	Burby *et al.* (2018)
PEB355	$\Delta ctpA$	(Burby *et al.* (2018)
PEB357	$\Delta ddcA$ (*ysoA*)	Burby *et al.* (2018)
PEB433	$\Delta yneA$::*erm*	Burby *et al.* (2018)
PEB439	$\Delta yneA$::*loxP*	Burby *et al.* (2018)
PEB495	$\Delta ddcA, \Delta yneA$::*erm*	This study
PEB497	$\Delta uvrAB, \Delta ddcA$	This study
PEB499	$\Delta ddcP, \Delta ddcA$	This study
PEB503	$\Delta ddcA, amyE$::P_{xyl}-*ddcA*	This study
PEB555	$\Delta ddcP, \Delta ctpA$	Burby *et al.* (2018)
PEB557	$\Delta ddcP, \Delta ctpA, amyE$::$P_{xyl}$-*ddcP*	Burby *et al.* (2018)
PEB561	$\Delta ddcP, \Delta ctpA, \Delta yneA$::*loxP*	Burby *et al.* (2018)
PEB579	$\Delta ctpA, \Delta ddcA$	This study
PEB587	$\Delta ddcA, \Delta yneA$::*loxP*	This study
PEB619	$\Delta ddcP, \Delta ctpA, amyE$::$P_{xyl}$-*ctpA*	Burby *et al.* (2018)
PEB639	$\Delta ddcP, \Delta ctpA, \Delta ddcA$	This study
PEB643	$\Delta ddcP, \Delta ctpA, \Delta ddcA, \Delta yneA$::*loxP*	This study
PEB719	$\Delta ddcP, amyE$::P_{xyl}-*ddcP*ΔTM	This study
PEB772	$\Delta ctpA, amyE$::P_{xyl}-*ctpA*ΔTM	This study
PEB774	*ddcP*ΔPDZ	This study
PEB776	*ctpA*ΔPDZ	This study
PEB836	$\Delta ddcA, amyE$::P_{xyl}-*ddcP*	This study
PEB837	$\Delta ddcA, amyE$::P_{xyl}-*ctpA*	This study
PEB838	$\Delta ddcP, \Delta ctpA, amyE$::$P_{xyl}$-*ddcA*	This study
PEB839	$\Delta ddcP, \Delta ctpA, \Delta ddcA, amyE$::$P_{xyl}$-*ddcP*	This study
PEB840	$\Delta ddcP, \Delta ctpA, \Delta ddcA, amyE$::$P_{xyl}$-*ddcA*	This study
PEB841	$\Delta ddcP, \Delta ctpA, \Delta ddcA, amyE$::$P_{xyl}$-*ctpA*	This study
PEB846	$amyE$::P_{xyl}-*yneA*	This study
PEB848	$\Delta ddcA, amyE$::P_{xyl}-*yneA*	This study
PEB850	$\Delta ddcP, \Delta ctpA, amyE$::$P_{xyl}$-*yneA*	This study
PEB852	$\Delta ddcP, \Delta ctpA, \Delta ddcA, amyE$::$P_{xyl}$-*yneA*	This study
PEB854	$\Delta ddcA, amyE$::P_{xyl}-*gfp-ddcA*	This study
PEB856	$\Delta ddcA, amyE$::P_{xyl}-*ddcA-gfp*	This study
PEB876	$amyE$::P_{xyl}-*gfp-yneA*	This study
PEB882	$\Delta ddcA, amyE$::P_{xyl}-*gfp-yneA*	This study
PEB888	$\Delta ddcP, \Delta ctpA, amyE$::$P_{xyl}$-*gfp-yneA*	This study
PEB894	$\Delta ddcP, \Delta ctpA, \Delta ddcA,$ $amyE$::P_{xyl}-*gfp-yneA*	This study

instructions. Membranes were blocked in 5% milk in TBST for 1 h at room temperature. Membranes were incubated with YneA antiserum at a 1:3000 dilution in 2% milk in TBST for 2 h at room temperature or at 4°C overnight. Membranes were washed 3 times with TBST for 5 min each and secondary antibodies (LiCor goat anti-Rabbit-680LT; 1:15000) were added and incubated for 1 h at room temperature. Membranes were washed 3 times with TBST for 5 min each. Images of membranes were captured using the LiCor Odyssey.

For overexpression of YneA, cultures of LB were inoculated at an $OD_{600} = 0.05$ and incubated at 30°C until an OD_{600} of about 0.2 (about 90 min). Xylose was added to 0.1% and cultures were incubated at 30°C for 2 h. Samples of an $OD_{600} = 25$ were harvested and re-suspended in 500 μL of sonication buffer as above. All subsequent steps were performed as described above.

For GFP-DdcA and DdcA-GFP, samples of an $OD_{600} = 1$ were harvested from LB + 0.05% xylose cultures via centrifugation and washed twice with 1× PBS pH 7.4. Samples were re-suspended in 100 μL 1× SMM buffer (0.5 M sucrose,

0.02 M maleic acid, 0.02 M MgCl$_2$, adjusted to pH 6.5) containing 1 mg/mL lysozyme and 2× Roche protease inhibitors. Samples were incubated at room temperature for 1 h and SDS sample buffer was added to 1× and incubated at 100°C for 7 min. Samples (10 μL) were separated via 10% or 4-20% SDS-PAGE. All subsequent steps were as described above, except GFP antisera (lot 1360-ex) was used at a 1:5000 dilution at 4°C overnight.

YneA stability assay

Cultures of LB were inoculated at an $OD_{600} = 0.05$ and incubated at 30°C until an OD_{600} of about 0.2 (about 90 min). Xylose was added to 0.1% and cultures were incubated at 30°C for 2 h. To stop translation, erythromycin was added to 50 μg/mL and samples ($OD_{600} = 10$) were taken at 0, 60, 120 and 180 min (the strains for this experiment contain the chloramphenicol resistant gene, *cat*, which prevents chloramphenicol from being used). Western blotting was performed as described above.

Subcellular fractionation

Fractionation experiments were performed as described previously (Wu and Errington, 1997). A cell pellet equivalent to 1 mL OD_{600} = 1 was harvested via centrifugation (10,000 *g* for 5 min at room temperature), and washed with 250 µL of 1× PBS. Protoplasts were generated by resuspension in 100 µL of 1× SMM buffer (0.5 M sucrose, 0.02 M maleic acid, 0.02 M $MgCl_2$, adjusted to pH 6.5) containing 1 mg/mL lysozyme and 1× Roche protease inhibitors at room temperature for 2 h. Protoplasts were pelleted via centrifugation: 5,000 *g* for 6 min at room temperature. Protoplasts were re-suspended in 100 µL of TM buffer (20 mM Tris, pH 8.0, 5 mM $MgCl_2$, 40 units/mL DNase I (NEB), 200 µg/mL RNase A (Sigma), 0.5 mM $CaCl_2$ and 1× Roche protease inhibitors) and left at room temperature for 30 min. The membrane fraction was pelleted via centrifugation: 20,800 *g* for 30 min at 4°C. The cytosolic fraction (supernatant) was transferred to a new tube and placed on ice, and the pellet was washed with 100 µL of TM buffer and pelleted via centrifugation as above. The supernatant was discarded and the pellet was re-suspended in 120 µL of 1× SDS dye. SDS loading dye was added to 1× to the cytosolic fraction and 12 µL of each fraction were used for Western blot analysis.

Culture supernatant protein precipitation

Culture supernatants were concentrated by TCA precipitation as described previously with minor modifications (Link and LaBaer, 2011). A culture was grown at 30°C until OD_{600} about 1, and the cells were pelleted via centrifugation: 7,000 *g* for 10 min at room temperature. The culture supernatant (30 mL) was filtered using a 0.22 µm filter and placed on ice. Proteins were precipitated by addition of 6 mL of ice-cold 100% TCA (6.1N), and left on ice for 30 min. Precipitated proteins were pelleted via centrifugation: 18,000 rpm (Sorvall SS-34 rotor) for 30 min at 4°C. Pellets were washed with 1 mL of ice-cold acetone and pelleted again via centrifugation: 20,000 *g* for 15 min at 4°C. The supernatant was discarded, and the residual acetone was evaporated by placing tubes in 100°C heat block for 1-2 min. Protein pellets were re-suspended in 120 µL of 6× SDS-loading dye and 12 µL were used in Western blot analysis.

Proteinase K sensitivity assay

Proteinase K sensitivity assays were performed similar to previous reports (Navarre and Schneewind, 1994; Wilson *et al*., 2012). A cell pellet from 0.5 mL OD_{600} = 1 equivalent was harvested and washed as in 'subcellular fractionation'. Protoplasts were generated by resuspension in 36 µL of 1× SMM buffer (0.5 M sucrose, 0.02 M maleic acid, 0.02 M $MgCl_2$, adjusted to pH 6.5) containing 1 mg/mL lysozyme at room temperature for 1 h. Either 9 µL of 1× SMM buffer or 0.5 mg/mL proteinase K (dissolved in 1× SMM buffer) was added (final proteinase K concentration of 100 µg/mL) and incubated at 37°C for the time indicated in the figures. Reactions were stopped by the addition of 5 µL of 50 mM PMSF (final concentration of 5 mM) and 25 µL of 6× SDS-dye (final concentration of 2×). For western blot analysis, 12 µL were used.

Microscopy

Strains were grown on LB agar plates containing 5 µg/mL chloramphenicol at 30°C overnight. For GFP-DdcA and DdcA-GFP, LB agar plates were washed with $S7_{50}$ media containing 1% arabinose and cultures of $S7_{50}$ media containing 1% arabinose and 0.05% xylose were inoculated at an OD_{600} = 0.1 and incubated at 30°C until an OD_{600} of about 0.4. Samples were taken and incubated with 2 µg/mL FM4-64 for 5 min and transferred to pads of 1× Spizizen salts and 1% agarose. Images were captured with an Olympus BX61 microscope using 250 ms and 1000 ms of exposure times for FM4-64 (membranes) and GFP, respectively. The brightness and contrast were adjusted for FM4-64 images with adjustments applied to the entire image. Strains with GFP-YneA were grown on LB agar plates containing 5 µg/mL chloramphenicol overnight at 30°C. Plates were washed with $S7_{50}$ minimal media containing 1% arabinose and cultures started at an OD_{600} = 0.1. Cultures were grown at 30°C until an OD_{600} of about 0.3 and xylose was added to 0.1%. Cultures were grown for 30 min at 30°C and imaged as for GFP-DdcA with exposure times of 300 ms for FM4-64 and 500 ms for GFP.

Author contributions

The study was conceived and designed by P.E.B. and L.A.S. Experiments were performed by P.E.B. and Z.W.S. Data analysis was performed by P.E.B., Z.W.S. and L.A.S. The manuscript was written and revised by P.E.B. and L.A.S.

References

Anderson, D.G. and Kowalczykowski, S.C. (1997) The translocating RecBCD enzyme stimulates recombination by directing RecA protein onto ssDNA in a chi-regulated manner. *Cell*, **90**, 77–86.

Au, N., Kuester-Schoeck, E., Mandava, V., Bothwell, L.E., Canny, S.P., Chachu, K. *et al*. (2005) Genetic composition of the *Bacillus subtilis* SOS system. *Journal of Bacteriology*, **187**, 7655–7666.

Bendtsen, J.D., Kiemer, L., Fausboll, A. and Brunak, S. (2005) Non-classical protein secretion in bacteria. *BMC Microbiology*, **5**, 58–71.

Bi, E. and Lutkenhaus, J. (1993) Cell division inhibitors SulA and MinCD prevent formation of the FtsZ ring. *Journal of Bacteriology*, **175**, 1118–1125.

Bojer, M.S., Wacnik, K., Kjelgaard, P., Gallay, C., Bottomley, A.L., Cohn, M.T. *et al*. (2018) SosA inhibits cell division in *Staphylococcus aureus* in response to DNA damage. *bioRxiv*, 1–39.

Buist, G., Steen, A., Kok, J. and Kuipers, O.P. (2008) LysM, a widely distributed protein motif for binding to (peptido) glycans. *Molecular Microbiology*, **68**, 838–847.

Burby, P.E. and Simmons, L.A. (2017) MutS2 promotes homologous recombination in *Bacillus subtilis*. *Journal of Bacteriology*, **199**, 1–13.

Burby, P.E., Simmons, Z.W., Schroeder, J.W. and Simmons, L.A. (2018) Discovery of a dual protease mechanism that promotes DNA damage checkpoint recovery. *PLOS Genetics*, **14**, e1007512.

Buttner, K., Bernhardt, J., Scharf, C., Schmid, R., Mader, U., Eymann, C. *et al.* (2001) A comprehensive two-dimensional map of cytosolic proteins of *Bacillus subtilis*. *Electrophoresis*, **22**, 2908–2935.

Canceill, D., Dervyn, E. and Huisman, O. (1990) Proteolysis and modulation of the activity of the cell division inhibitor SulA in *Escherichia coli* lon mutants. *Journal of Bacteriology*, **172**, 7297–7300.

Cerveny, L., Straskova, A., Dankova, V., Hartlova, A., Ceckova, M., Staud, F. *et al.* (2013) Tetratricopeptide repeat motifs in the world of bacterial pathogens: role in virulence mechanisms. *Infection and Immunity*, **81**, 629–635.

Chauhan, A., Lofton, H., Maloney, E., Moore, J., Fol, M., Madiraju, M.V. *et al.* (2006) Interference of *Mycobacterium tuberculosis* cell division by Rv2719c, a cell wall hydrolase. *Molecular Microbiology*, **62**, 132–147.

Churchill, J.J., Anderson, D.G. and Kowalczykowski, S.C. (1999) The RecBC enzyme loads RecA protein onto ssDNA asymmetrically and independently of chi, resulting in constitutive recombination activation. *Genes & Development*, **13**, 901–911.

Claessen, D., Emmins, R., Hamoen, L.W., Daniel, R.A., Errington, J. and Edwards, D.H. (2008) Control of the cell elongation-division cycle by shuttling of PBP1 protein in *Bacillus subtilis*. *Molecular Microbiology*, **68**, 1029–1046.

Daniel, R.A. and Errington, J. (2003) Control of cell morphogenesis in bacteria: two distinct ways to make a rod-shaped cell. *Cell*, **113**, 767–776.

Donachie, W.D. and Blakely, G.W. (2003) Coupling the initiation of chromosome replication to cell size in *Escherichia coli*. *Current Opinion in Microbiology*, **6**, 146–150.

Erill, I., Campoy, S. and Barbe, J. (2007) Aeons of distress: an evolutionary perspective on the bacterial SOS response. *FEMS Microbiology Reviews*, **31**, 637–656.

Eymann, C., Dreisbach, A., Albrecht, D., Bernhardt, J., Becher, D., Gentner, S. *et al.* (2004) A comprehensive proteome map of growing *Bacillus subtilis* cells. *Proteomics*, **4**, 2849–2876.

Friedberg, E.C., Walker, G.C., Siede, W., Wood, R.D., Schultz, R.A. and Ellenberger, T. (2006) *DNA Repair and Mutagenesis*, 2nd edition. Washington, DC: ASM Press.

Gibson, D.G. (2011) Enzymatic assembly of overlapping DNA fragments. In: Voigt, C. (Ed.) *Synthetic Biology, Pt B: Computer Aided Design and DNA Assembly*, **498**. San Diego: Elsevier Academic Press Inc, pp. 349–361.

Goranov, A.I., Katz, L., Breier, A.M., Burge, C.B. and Grossman, A.D. (2005) A transcriptional response to replication status mediated by the conserved bacterial replication protein DnaA. *Proceedings of the National Academy of Sciences USA*, **102**, 12932–12937.

Goranov, A.I., Kuester-Schoeck, E., Wang, J.D. and Grossman, A.D. (2006) Characterization of the global transcriptional responses to different types of DNA damage and disruption of replication in *Bacillus subtilis. Journal of Bacteriology*, **188**, 5595–5605.

Hill, N.S., Kadoya, R., Chattoraj, D.K. and Levin, P.A. (2012) Cell size and the initiation of DNA replication in bacteria. *PLoS Genetics*, **8**, e1002549.

Hirose, I., Sano, K., Shioda, I., Kumano, M., Nakamura, K. and Yamane, K. (2000) Proteome analysis of *Bacillus subtilis* extracellular proteins: a two-dimensional protein electrophoretic study. *Microbiology*, **146**, 65–75.

Hofmann, K. and Stoffel, W. (1993) TMBASE – a database of membrane spanning protein segments. *Biological Chemistry Hoppe Seyler*, **347**, 166–174.

Huang, J., Cao, C. and Lutkenhaus, J. (1996) Interaction between FtsZ and inhibitors of cell division. *Journal of Bacteriology*, **178**, 5080–5085.

Huisman, O. and D'Ari, R. (1981) An inducible DNA replication-cell division coupling mechanism in *E. coli. Nature*, **290**, 797–799.

Huisman, O., D'Ari, R. and Gottesman, S. (1984) Cell-division control in *Escherichia coli*: specific induction of the SOS function SfiA protein is sufficient to block septation. *Proceedings of the National Academy of Sciences USA*, **81**, 4490–4494.

Ivancic-Bace, I., Peharec, P., Moslavac, S., Skrobot, N., Salaj-Smic, E. and Brcic-Kostic, K. (2003) RecFOR function is required for DNA repair and recombination in a RecA loading-deficient recB mutant of *Escherichia coli. Genetics*, **163**, 485–494.

Ivancic-Bace, I., Vlasic, I., Salaj-Smic, E. and Brcic-Kostic, K. (2006) Genetic evidence for the requirement of RecA loading activity in SOS induction after UV irradiation in *Escherichia coli. Journal of Bacteriology*, **188**, 5024–5032.

Iyer, V.N. and Szybalski, W. (1963) A molecular mechanism of mitomycin action: Linking of complementary DNA strands. *Proceedings of the National Academy of Sciences USA*, **50**, 355–362.

Kanemori, M., Yanagi, H. and Yura, T. (1999) The ATP-dependent HslVU/ClpQY protease participates in turnover of cell division inhibitor SulA in *Escherichia coli. Journal of Bacteriology*, **181**, 3674–3680.

Kawai, Y., Moriya, S. and Ogasawara, N. (2003) Identification of a protein, YneA, responsible for cell division suppression during the SOS response in *Bacillus subtilis. Molecular Microbiology*, **47**, 1113–1122.

Kreuzer, K.N. (2013) DNA damage responses in prokaryotes: regulating gene expression, modulating growth patterns, and manipulating replication forks. *Cold Spring Harbor Perspectives in Biology*, **5**, a012674.

Krogh, A., Larsson, B., von Heijne, G. and Sonnhammer, E.L. (2001) Predicting transmembrane protein topology with a hidden Markov model: application to complete genomes. *Journal of Molecular Biology*, **305**, 567–580.

Kross, J., Henner, W.D., Hecht, S.M. and Haseltine, W.A. (1982) Specificity of deoxyribonucleic acid cleavage by bleomycin, phleomycin, and tallysomycin. *Biochemistry*, **21**, 4310–4318.

Lenhart, J.S., Schroeder, J.W., Walsh, B.W. and Simmons, L.A. (2012) DNA repair and genome maintenance in *Bacillus subtilis. Microbiology and Molecular Biology Reviews*, **76**, 530–564.

Lewis, L.K., Harlow, G.R., Gregg-Jolly, L.A. and Mount, D.W. (1994) Identification of high affinity binding sites for

LexA which define new DNA damage-inducible genes in *Escherichia coli*. *Journal of Molecular Biology*, **241**, 507–523.

Link, A.J. and LaBaer, J. (2011) Trichloroacetic acid (TCA) precipitation of proteins. *Cold Spring Harbor Protocols*, **2011**, 993–994.

Little, J.W. and Mount, D.W. (1982) The SOS regulatory system of *Escherichia coli*. *Cell*, **29**, 11–22.

Little, J.W., Mount, D.W. and Yanisch-Perron, C.R. (1981) Purified lexA protein is a repressor of the recA and lexA genes. *Proceedings of the National Academy of Sciences USA*, **78**, 4199–4203.

Mizusawa, S. and Gottesman, S. (1983) Protein degradation in *Escherichia coli*: the lon gene controls the stability of sulA protein. *Proceedings of the National Academy of Sciences USA*, **80**, 358–362.

Mo, A.H. and Burkholder, W.F. (2010) YneA, an SOS-induced inhibitor of cell division in *Bacillus subtilis*, is regulated posttranslationally and requires the transmembrane region for activity. *Journal of Bacteriology*, **192**, 3159–3173.

Modell, J.W., Hopkins, A.C. and Laub, M.T. (2011) A DNA damage checkpoint in *Caulobacter crescentus* inhibits cell division through a direct interaction with FtsW. *Genes & Development*, **25**, 1328–1343.

Modell, J.W., Kambara, T.K., Perchuk, B.S. and Laub, M.T. (2014) A DNA damage-induced, SOS-independent checkpoint regulates cell division in *Caulobacter crescentus*. *PLoS Biology*, **12**, e1001977.

Morimatsu, K. and Kowalczykowski, S.C. (2003) RecFOR proteins load RecA protein onto gapped DNA to accelerate DNA strand exchange: a universal step of recombinational repair. *Molecular Cell*, **11**, 1337–1347.

Mukherjee, A., Cao, C. and Lutkenhaus, J. (1998) Inhibition of FtsZ polymerization by SulA, an inhibitor of septation in *Escherichia coli*. *Proceedings of the National Academy of Sciences USA*, **95**, 2885–2890.

Navarre, W.W. and Schneewind, O. (1994) Proteolytic cleavage and cell wall anchoring at the LPXTG motif of surface proteins in gram-positive bacteria. *Molecular Microbiology*, **14**, 115–121.

Noll, D.M., Mason, T.M. and Miller, P.S. (2006) Formation and repair of interstrand cross-links in DNA. *Chemical Reviews*, **106**, 277–301.

Ogino, H., Teramoto, H., Inui, M. and Yukawa, H. (2008) DivS, a novel SOS-inducible cell-division suppressor in *Corynebacterium glutamicum*. *Molecular Microbiology*, **67**, 597–608.

Reiter, H., Milewskiy, M. and Kelley, P. (1972) Mode of action of phleomycin on *Bacillus subtilis*. *Journal of Bacteriology*, **111**, 586–592.

Sancar, A. (1996) DNA excision repair. *Annual Review of Biochemistry*, **65**, 43–81.

Scheffers, D.J. and Errington, J. (2004) PBP1 is a component of the *Bacillus subtilis* cell division machinery. *Journal of Bacteriology*, **186**, 5153–5156.

Seong, I.S., Oh, J.Y., Yoo, S.J., Seol, J.H. and Chung, C.H. (1999) ATP-dependent degradation of SulA, a cell division inhibitor, by the HslVU protease in *Escherichia coli*. *FEBS Letters*, **456**, 211–214.

Slilaty, S.N. and Little, J.W. (1987) Lysine-156 and serine-119 are required for LexA repressor cleavage: a possible mechanism. *Proceedings of the National Academy of Sciences USA*, **84**, 3987–3991.

Smith, D.F. (2004) Tetratricopeptide repeat cochaperones in steroid receptor complexes. *Cell Stress Chaperones*, **9**, 109–121.

Sonezaki, S., Ishii, Y., Okita, K., Sugino, T., Kondo, A. and Kato, Y. (1995) Overproduction and purification of SulA fusion protein in *Escherichia coli* and its degradation by Lon protease in vitro. *Applied Microbiology and Biotechnology*, **43**, 304–309.

Tiyanont, K., Doan, T., Lazarus, M.B., Fang, X., Rudner, D.Z. and Walker, S. (2006) Imaging peptidoglycan biosynthesis in *Bacillus subtilis* with fluorescent antibiotics. *Proceedings of the National Academy of Sciences USA*, **103**, 11033–11038.

Tjalsma, H., Bolhuis, A., Jongbloed, J.D., Bron, S. and van Dijl, J.M. (2000) Signal peptide-dependent protein transport in *Bacillus subtilis*: a genome-based survey of the secretome. *Microbiology and Molecular Biology Reviews*, **64**, 515–547.

Trusca, D., Scott, S., Thompson, C. and Bramhill, D. (1998) Bacterial SOS checkpoint protein SulA inhibits polymerization of purified FtsZ cell division protein. *Journal of Bacteriology*, **180**, 3946–3953.

Wang, J.D. and Levin, P.A. (2009) Metabolism, cell growth and the bacterial cell cycle. *Nature Reviews Microbiology*, **7**, 822–827.

Westfall, C.S. and Levin, P.A. (2017) Bacterial cell size: multifactorial and multifaceted. *Annual Review of Microbiology*, **71**, 499–517.

Wilson, M.J., Carlson, P.E., Janes, B.K. and Hanna, P.C. (2012) Membrane topology of the *Bacillus anthracis* GerH germinant receptor proteins. *Journal of Bacteriology*, **194**, 1369–1377.

Wu, L.J. and Errington, J. (1997) Septal localization of the SpoIIIE chromosome partitioning protein in *Bacillus subtilis*. *The EMBO Journal*, **16**, 2161–2169.

Wu, W.F., Zhou, Y. and Gottesman, S. (1999) Redundant in vivo proteolytic activities of *Escherichia coli* Lon and the ClpYQ (HslUV) protease. *Journal of Bacteriology*, **181**, 3681–3687.

Youngman, P., Perkins, J.B. and Losick, R. (1984) Construction of a cloning site near one end of TN917 into which foreign DNA may be inserted without affecting transposition in *Bacillus subtilis* or expression of the transposon-bourne ERM gene. *Plasmid*, **12**, 1–9.

Yu, N.Y., Wagner, J.R., Laird, M.R., Melli, G., Rey, S., Lo, R. *et al.* (2010) PSORTb 3.0: improved protein subcellular localization prediction with refined localization subcategories and predictive capabilities for all prokaryotes. *Bioinformatics*, **26**, 1608–1615.

Supporting Information

Additional supporting information may be found online in the Supporting Information section at the end of the article.